

Ductile-Regime Turning of Germanium and Silicon

by

Peter N. Blake,
Fabrication Engineering Branch
Goddard Space Flight Center
Greenbelt, MD 20771

and

Ronald O. Scattergood,
Precision Engineering Center
North Carolina State University
Raleigh, NC 27695-7918

(NASA-TM-101231) DUCTILE-REGIME TURNING OF
GERMANIUM AND SILICON (NASA) 22 p CSCL 13H

N89-20322

Unclas
G3/31 0191657

ABSTRACT

Single-point diamond turning of silicon and germanium was investigated in order to clarify the role of cutting depth in coaxing a ductile chip formation in normally brittle substances. Experiments based on the rapid withdrawal of the tool from the workpiece have shown that microfracture damage is a function of the effective depth of cut (as opposed to the nominal cutting depth). In essence, damage created by the leading edge of the tool is removed several revolutions later by lower sections of the tool edge, where the effective cutting depth is less. It appears that a truly ductile cutting response can be achieved only when the effective cutting depth, or critical chip thickness, is less than about 200nm . Factors such as tool rake angle are significant in that they will affect the actual value of the critical chip thickness for transition from brittle to ductile response. It is concluded that the critical chip thickness is an excellent parameter for measuring the effects of machining conditions on the ductility of the cut and for designing tool-workpiece geometry in both turning and grinding.

INTRODUCTION

When silicon and germanium are tested at room temperature in tension, uniaxial compression, or bending, they are brittle. They fracture before any permanent measureable plastic deformation

occurs. One concludes that their fracture strength is lower than their yield strength, and that a uniaxial yield stress is not obtainable from these tests.

The fundamental hypotheses of this research program is that as the scale of deformation decreases, plastic deformation becomes more energetically favorable than fracture, and that there is in fact a critical value of deformation depth, d , at which the favored deformation process switches from fracture to plasticity. A simple model has been developed (1) which relates the critical depth, d , to material parameters, as follows:

$$d = d_{crit} \propto \left(\frac{K_c}{H} \right)^2 \quad (1)$$

where K_c is the fracture toughness and H is the hardness. The constant of proportionality must be calibrated experimentally. The present work in progress attempts to find this critical depth as a function of machining parameters in germanium and silicon.

A brittle--ductile transition at small volumes has been seen in other contexts. Davis and Koch (2) report that when germanium and silicon are milled together in a ball mill, there is a lower limit to the size of the resulting powders; and at this size particle, the silicon and germanium are alloyed in complete solid solution, having been mechanically (plastically) deformed together into intimate mixture. The particles are frequently bonded together by necks. Apparently, there is a particle volume below which fracture does not occur.

A size effect in fracture strength has also been demonstrated by Ikawa and Shimada (3), this time in diamond. A diamond indenter was placed in Hertzian contact with a polished diamond sample. As the indenter radius was decreased from $500\mu m$ to $5\mu m$, the radial stress achievable before fracture in Hertzian contact rose four-fold and approached the magnitude of the theoretical value, $E/10$ (where E is Young's modulus). This result is important to the discussion because it points out that very large stresses can be achieved in small scale deformations. There is a common perception that dislocations cannot move at room temperature in silicon; but, surely, they can, if the shear stress is high enough. And there is an upper limit to this stress: the theoretical maximum shear stress,

$G/10$ (where G is the shear modulus). The theoretical maximum shear stress is the calculated stress necessary to shear the whole crystal plane of atoms, without the benefit of the dislocation mechanism. In other words, if cracking can be prevented, ductile deformation will occur.

MACHINE REQUIREMENTS

The laboratory-scale diamond-turning machine used in this study is known as the Parallel Axis Ultra-Precision Lathe (PAUL) and was designed and built in the Precision Engineering Center (4). The requirements for experimentation in ductile regime machining of hard materials are low cutting forces, high machine rigidity, and precise control of tool infeed to give small chip removal thicknesses. In addition to the need for an actuator with high resolution, the effects of thermal drift, vibration, and spindle runout must be reduced to acceptable levels or compensated.

For stiffness and low runout, the machine uses hydrostatic air bearings

(Professional Instruments: 4in. "Blockhead") for both the workpiece rotation and the tool arm travel. These bearings exhibit less than 50nm axial or radial runout, with most of this error motion being a repeated, once-per-revolution error. The machine has an axial stiffness of $8.8 \times 10^6 N/m$ at the point of tool contact. The workpiece is rotated on a vertical axis air-bearing spindle, and the tool holder is mounted on a second vertical axis spindle, instead of a linear slide. Driven slowly, this allows the tool to sweep across the face of the workpiece, towards its center. The tool can be adjusted vertically with the piezoelectric stack (PZT) to control the depth of cut; and the tool arm is driven horizontally at controllable feed rates with a micro-positioner (the Oriel Motormike).

To eliminate thermal expansion problems, the machine is located in a temperature controlled room regulated to ± 0.05 deg C. For vibration elimination, PAUL is mounted on a vibration isolation table that effectively attenuates environmental disturbances above five Hertz.

SINGLE-POINT DIAMOND TURNING

The present project attempts to find the critical depth for ductile-regime turning of silicon and germanium at room temperature. The tool used is made of single-crystal gem quality

diamond, sharpened to an edge formed between a flat rake face, called the table, and the clearance surface. Looked at from the front of the rake face, the cutting edge has the shape of a circular arc, called the *nose* (Fig 1). The nose radius is on the order of millimeters. The *edge radius*, however, is very small; and one of the reasons for using single-crystal, gem-quality diamond for the tool material is that it can be polished to an edge radius that is, at the present time, unmeasurable, but is thought to be under 100 Å (5).

The turning procedure used is known as facing, wherein the workpiece is rotated and the tool is moved in a straight line radially inwards to the center, cutting a spiral groove so tightly spaced that the surface remaining is flat and smooth to less than 0.1 micrometers (Fig 2).

The chip formation process for the ductile regime (Fig. 3) is envisioned as in the well-known orthogonal model of Merchant (6). In the orthogonal model, the chip thickness and stress profile are constant across the third dimension, the chip width. In diamond-turning, the chip thickness varies linearly and slowly across the chip width, giving an approximation of orthogonal conditions from a micromechanics point of view, but giving a radically differently shaped chip form. The geometry of single-point turning with a circular-nosed tool allows the removal of chips with a thickness one to two orders of magnitude smaller than either the depth of cut or the feed per revolution. Thus the spindles can have a run-out of about 50nm superimposed on a depth of cut of 2.5µm and a feed per revolution of 2.5µm; and the maximum chip thickness will still be stable at 100 ± 10nm. This geometrical relation will be shown below.

The cross-section of the undeformed chip of a finish cut is shown in Figure 4. This view is along a direction parallel to the cutting path and shows that the thickness of the cut varies almost linearly across the cross-sectional width of the chip. The undeformed chip thickness, *t*, is given as a function of this distance, *x*, where *x* is the lateral distance from the end of the cut in the finish surface: (f=feed per revolution; R=tool nose radius; d=depth of cut)

$$t = \frac{fx}{R} \quad (2)$$

The maximum chip thickness is given by:

$$t_m = f \sqrt{\frac{2d}{R}} \quad (3)$$

The total cross-sectional chip width is given by:

$$W = \sqrt{2dR} \quad (4)$$

For example, in a typical cut with depth and feed both $2.5 \mu m$, and $R = 3.125 mm$, the maximum thickness of the undeformed chip is much less ($100nm$) than the depth of cut and the width of the chip is many times greater ($125\mu m$) than the feed. The tool will be removing material from above any point in the finish surface during each of its 50 passes over that point. The local chip thickness, t , is the parameter which will correspond to depth of cut in the orthogonal model and in discussion of critical depth of cut. Therefore, in all further discussion of the effect of scale on ductile-regime machining, the phrase *critical depth of cut* will be replaced by the phrase *critical chip thickness*.

PROCEDURE FOR TURNING EXPERIMENTS

Single-crystal, optical grade germanium (n-doped and dislocation concentration uncontrolled), obtained from Eagle-Picher in the form of sawn wafers of known crystal orientation and of diameter $63.5mm$ and $76.2mm$, was acid-etch-polished (with CP-4) for five minutes to remove $100\mu m$ of material from each side, in order to remove all previous saw damage. The wafers were mounted with heat-softening glue ($< 100^\circ C$) on $76.2mm$ (3 in.) circular aluminum and copper mounts, which were then mechanically chucked onto the face plate of the workpiece spindle of PAUL. The wafers were then to be turned (faced).

The room temperature was held to $20 \pm 0.05 deg C$. The coolant was distilled H_2O , delivered in two jet streams, one focused on the tool tip, and the other washing the whole surface. Each test surface was prepared with a series of seven facing cuts (rake = $-10 deg$), each cut to be half the depth of the previous cut, with a final

preparation cut of depth $0.5\mu m$ and feed $2\mu m/rev$. The test cuts followed. All test cuts were done with a fresh edge on specially dedicated tools, sharpened at Lawrence Livermore Laboratories. The three test tools had rake angles of $0\ deg$, $-10\ deg$, and $-30\ deg$, and a nose radius of $3.125mm$. Unless otherwise noted, the clearance angle was $6\ deg$ and the cutting speed was $2.1m/s$ ($5000in/min$).

Silicon samples, obtained from Wacker and from Monsanto, were lightly doped p-type and pre-polished. In most experiments, these were test-machined in the as-received state. Testing cuts were similar to those for germanium.

The standard test cut allowed 12-20 test conditions on each sample disk. For each condition, the tool was lowered slowly without radial feed into the workpiece (a plunge cut), then fed forward slowly at a feed of $1.25\mu m/rev$ (to smooth away damage from the plunge), fed forward at the test conditions and suddenly lifted by the PZT depth control out of the facing cut, leaving a slope or "shoulder"--the forward edge of the test cut. Figure 5 shows a low power oblique view of the finish surface and the shoulder of a deep cut. The tool was then advanced without cutting to the location where the next series was to begin.

The following list describes the values of cutting parameters investigated:

Depth, d:	from $0.12\mu m$ to $125\mu m$
Feed, f:	from $1.25\mu m$ to $10\mu m$
Rake :	0° , -10° , -30°
Clearance angle:	6° , 16°
Cutting speed:	0.84 , 2.1 , $14.3\ m/s$
Crystal orientation:	(100), (110), (111)

RESULTS AND DISCUSSION: CHIP FORMATION

Machining debris taken after a facing cut of germanium is shown in Figure 6. It can be seen that the debris is in the form of a continuous chip, and not in crushed or fractured powder. This continuity in itself is conclusive evidence of plasticity (ductility) in the deformation.

RESULTS AND DISCUSSION: GERMANIUM SURFACES

A typical surface finish on germanium turned on PAUL is $8\ \text{\AA}$ rms over a $100\ \mu m$ trace (Los Alamos Sommagren instrument). The low

roughness over this distance is a reflection of the chip formation process.

Damage can occur when certain cutting parameters are exceeded; a light-scattering, pitting damage is created in the surface. Under optimal conditions, the surface is smooth; no pits are left. Dimensions of the pits vary somewhat with the machining parameters, but lateral dimensions are on the order of 1-4 μm and the depths (measured roughly by stereoscopy in the SEM) are about an order of magnitude smaller than the widths.

The pitting damage in germanium occurs in radial sectors whose centers and borders can be described as crystal directions. Figure 7 shows a photograph of a sample with 10 test cutting conditions, several of which produced pitting in the radial sector described. On surfaces oriented on the (100), (110), and (111) planes, the pitting occurs when the tool is cutting within a few degrees of the $\langle 110 \rangle$ direction. For the (110) samples, pitting also occurs in the $\langle 100 \rangle$ direction. In 14 samples randomly set on the spindle, the average deviation of the estimated center of the pitting sector from the predicted crystal direction was 0.2 deg (range = ± 8 deg). The width of the pitting sector varied with cutting conditions, in the same way as did the size of the pits: deeper, higher feed cuts produced larger damage areas with bigger and more numerous pits, thus scattering more light.

Examination was made of the slope or "shoulder" left at the forward end of the cut when the tool is swiftly retracted up out of the surface. Figure 8, a SEM micrograph taken normal to the surface, shows that pitting occurs along most of the shoulder. Evidently, pitting occurs at the forward edge of the cut, where the local chip thickness is larger, and not at the trailing edge, where the thickness decreases to zero. In fact, in its many passes over one final spot on the surface, the tool removes damage previously created, so that the final 5, 10, or 20 passes remove all previous pitting damage. Figure 9 summarizes this idea.

It is clear that there is a significant range of chip thicknesses where both ductile removal and fracture take place. The damage seen is the punctuation of the material-removal process with brittle fracture events. Measurements by stereoscopic pairs were made of the depth of the pits. The pits at the leading edge of the shoulder are about 0.3 μm deep; they increase to 0.6 μm over the large area in the middle of the slope; they then decrease at the bottom to 20nm, then disappear.

Influence of Depth and Feed

Originally, it was hypothesized that the maximum chip thickness, t_m , would be the dominant parameter in determining whether the surface suffered pitting damage or not. But the understanding of pitting along the tool shoulder eliminates that hypothesis. The pits created at the point of maximum chip thickness are not very deep ($0.1-0.3\mu m$, compared to a depth of cut of $2-200\mu m$). Their creation would have little to do with the final surface.

More significant would be the chip thickness at the point along the tool shoulder where pits ceased to be created. It can be seen that the feed per revolution will have a dominant effect on the chip thickness. Figure 10 illustrates the effect of increasing depth of cut on the cross-sectional shape of the chip, and the effect of increased feed. Increased depth increases t_m , but merely by making the chip wider, leaving the relationship between chip thickness and distance along the chip width unchanged. However, increasing the feed increases the chip thickness along its whole width.

If pitting does indeed depend on the local chip thickness, and if there is a critical chip thickness at which pitting ceases, then the distance up the slope that pitting disappears, x_t (Fig 11), being proportional to the local chip thickness, should be inversely dependent on the feed. Figure 12 shows that this distance, x_t , depends in one sample exactly on the feed and not at all on the depth of cut. This figure is a montage/ comparison of micrographs of six conditions: three feeds, with two depths realized for each feed by slanting the sample on the spindle. The micrographs were taken along the $\langle 110 \rangle$ direction on two opposite sides of the disk, the high side and the low side. The micrographs were then positioned so that the bottoms of the tool shoulders in each photograph were aligned, and the distance up the slopes that pitting ceased could be compared. For each of the three feeds, this distance, x_t , is constant with changing depth of cut. But between the three feeds, there is a great difference in x_t ; x_t decreases with an increase in feed.

Critical Chip Thickness

Taking x_t as the primary datum, the chip thickness at the point where pitting ceases, y_t (Fig 11) can be easily calculated by equation 2. This parameter is an estimate of the critical maximum

chip thickness, t_c , which is defined as the maximum chip thickness, t_m , at which no pitting occurs at all during the cut, not even on the slope.

Measurements of x_t and y_t for trials of varying depth and feed are given in Table 1. The first point to be made is that x_t is not correlated with depth of cut, but is dependent on feed, as hypothesized, and varies in such a way that the parameter y_t is almost constant over varying feed; the variation is so small that satisfaction with y_t as an important parameter is strengthened. For a rake angle of 0 deg , the mean values of y_t vary only between 10 and 35 nm . The variation of y_t with feed for a 0 deg rake angle is shown in figure 13; y_t increases as the feed decreases. This variation of y_t with feed is what would be expected if existing pits extended below the level of the immediately succeeding tool pass, making it "hard" to clear away pits even at local chip thicknesses below t_c . It is concluded that y_t is a better estimate of t_c as the feed decreases, i.e., as the maximum chip thickness approaches the critical chip thickness.

In order to compare the influence of other variables in the further experiments reported here, however, the critical chip thickness is estimated by y_t at a standardized feed, chosen to be $f = 2.5 \mu m/rev$.

Influence of Rake Angle

Using y_t ($f=2.5 \mu m$) as a measure of the influence of rake angle (Fig 14), we find that for a rake angle of 0 deg , the mean y_t is 20 nm ($s= 2$); for -10 deg , the mean y_t is 12 nm ($s= 5$); and for a rake angle of -30 deg , the mean y_t is 200 nm ($s=35$). For rake angles of 0 deg and -10 deg , the measures of y_t are not significantly different; but for -30 deg , y_t is much larger.

Influence of Cutting Speed

A sequence of varied cutting speeds was repeated on two germanium workpieces. Unfortunately, these samples showed the signs of an undesired feed variation error. Due to the strong dependence of y_t on feed, it was not possible to use y_t as a measure of the effect of cutting speed. An alternate measure of pitting damage is the area density of pits in the finished surface. In figure 15 are shown finish surfaces with pits present, trials in which,

clearly, there were no measurements of y_t . Six trials are shown, with cutting speeds of 2.1 m/s and 14.3 m/s factored with three feeds. The variation in feed occurred in cycles of shorter length than the trials, and each trial was affected equally by the feed variation. Comparing pit area density between speeds at each feed shows clearly that the trials at high speed had an improved surface. Ten more pairwise cutting speed comparisons were made at another rake angle (0 deg), all with the same result: increased cutting speed moderately decreased pitting damage .

RESULTS OF WORK IN PROGRESS; SILICON SURFACES

Pitting along the <110>

The pattern of pitting on the tool-retraction shoulder in germanium along the <110> appears in silicon also--with one difference: there is less of it, for a given feed. Given a rake of -30 deg and a feed of $f = 2.5 \mu m$, y_t is estimated at greater than 250 nm (compared to 175-200 nm for Ge). Pitting along the <110>, with its clear relations to feed and rake and its consistent spacial patterns, the major form of damage in germanium, was initially only a minor form of damage in the silicon samples tested.

Pitting along the <100>

A much more serious damage in silicon occurs predominantly along the <100> direction, but is not limited to this direction. It is a kind of spalling damage (Figure 16), which resembles the wear produced when a hard spherical ball or pin is drawn back-and-forth along a path on a silicon sample. A surface layer has spalled off, leaving a jumbled-looking surface beneath; the edges of the pit have been burnished into a lip. This spalling damage occurs in random bursts and shows only a mild relation to the feed. It shows no relation to position on the tool-lift shoulder.

It was hypothesized that this damage could occur when chips are dragged under the tool, rewelded to the surface, and torn off during the many passes of the tool. It could also be that extensive tool wear on the flank increases the extent of the wear land and produces this morphology in a crushing action. Both hypotheses suggested that a cure might be effected by increasing the back clearance angle of the tool. When the clearance angle was increased from 6 deg to 16 deg, the "spalling" damage along the <100> direction was

completely eliminated, while the pitting along the $\langle 110 \rangle$ was not eliminated (7).

Surface Roughness

The surfaces of silicon, even when unpitted, are rougher than those of germanium. The silicon surfaces also usually scatter white light in a "rainbow" effect. From experience in metal-cutting, this effect is known to be often due to tool wear causing nicks in the tool edge, causing ridges within the machining grooves. This rainbow effect is due to tool wear, which occurs at a much faster rate in silicon than in germanium.

SUMMARY

Pitting damage that occurs along the $\langle 110 \rangle$ direction in germanium and silicon can be removed by later revolutions of the workpiece during the same pass of the tool. The pits are removed by those sections of the tool edge that are forming a chip with thickness less than chip thickness, y_t . This critical thickness depends strongly on the rake angle and on the material, and only weakly on the cutting speed. For a rake angle of 0 deg to -10 deg , y_t for germanium is between 15 nm and 20 nm . For a rake angle of -30 deg , y_t is about 200 nm . For silicon with a rake angle of -30 deg , t_c is estimated to be greater than 250 nm .

A severe pitting damage of a different morphology occurs along the $\langle 100 \rangle$ direction of silicon. This damage can be eliminated--at least over the short test runs of the present experiment--by increasing the clearance angle from 6 deg to 16 deg .

Work in progress aims to solidify and define *critical chip thickness*, t_c , as an unambiguous, repeatable experimental parameter which can quantitatively indicate how far into or out of the ductile regime any certain set of machining parameters and material parameters leads. It can be the tool for rapidly determining the effects of these parameters and for designing new turning and grinding processes, with new tool-workpiece relations.

ACKNOWLEDGEMENT

The authors would like to acknowledge the support provided by the Office of Naval Research (contract no. ONR-N00014-86-K-0681) and the industrial sponsors of the Precision Engineering Center at North Carolina State University.

REFERENCES

1. Bifano, T. G., T.A. Dow, and R.O. Scattergood, "Ductile-Regime Grinding of Brittle Materials", *Proc. Conf. on Ultra-Precision in Manufacturing Engineering*, Aachen, W. Germany, 1988.
2. Davis, R.N., and C.L. Koch, *Scripta Metallurgica*, 21, pp 305-310, 1987.
3. Ikawa, N. and S. Shimada, "Microstrength Measurement of Brittle Materials", *Technology Reports of the Osaka University*, Vol. 31, No. 1622, p. 315, 1981 .
4. Falter, P. J. and T. A. Dow, "Design and Testing of a Small Scale Diamond Turning Machine." *Precision Engineering*,9 (4), pp185-190, 1987.
5. Ikawa, N. and S. Shimada, "Cutting Tool for Ultraprecision Machining," *Proceedings 3rd Int. Conf. on Production Engineering, Kyoto*. Sponsored by the Japan Society of Precision Engineering, 1977.
6. Shaw, M.C., *Metal Cutting Principles*, Clarendon Press, Oxford, 1984
7. Blake, P.N., *Ductile-Regime Turning of Germanium and Silicon*, PhD thesis, North Carolina State University, 1988.

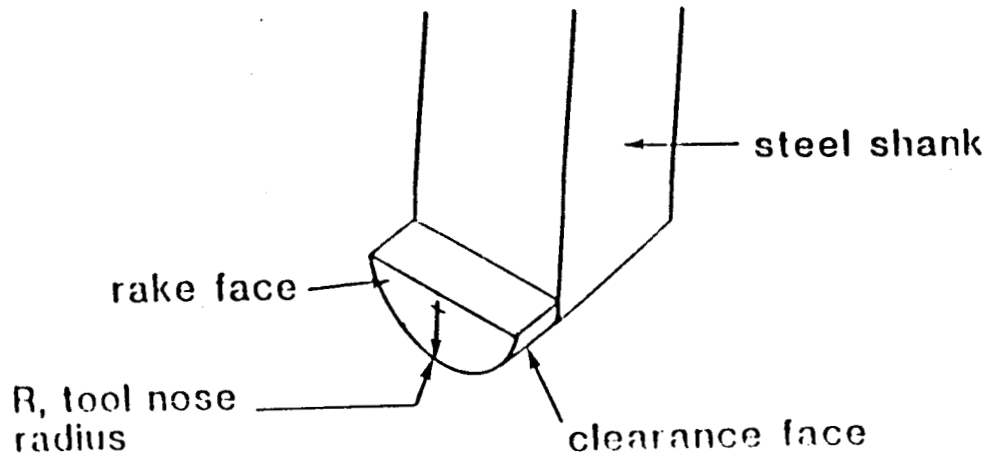


Fig. 1 The diamond tool

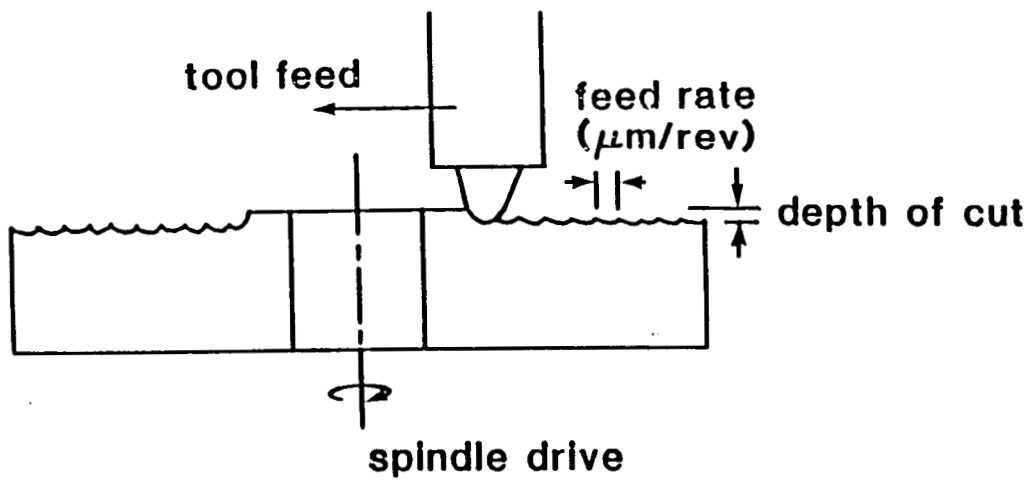


Fig. 2 The facing process

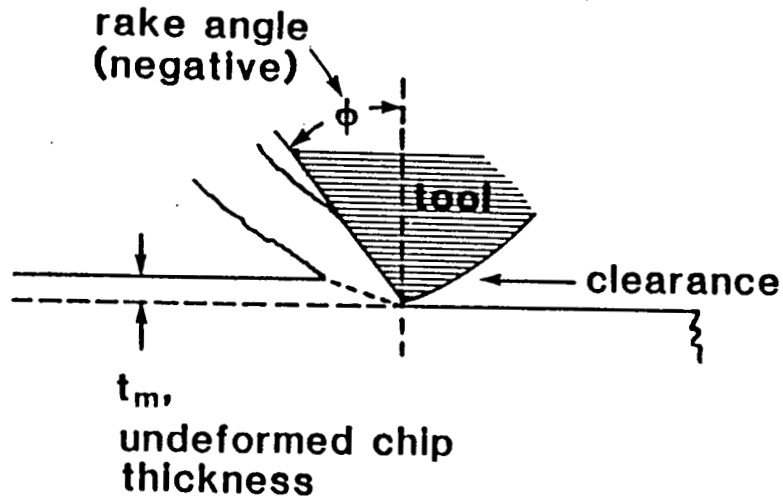


Fig. 3 Chip formation process

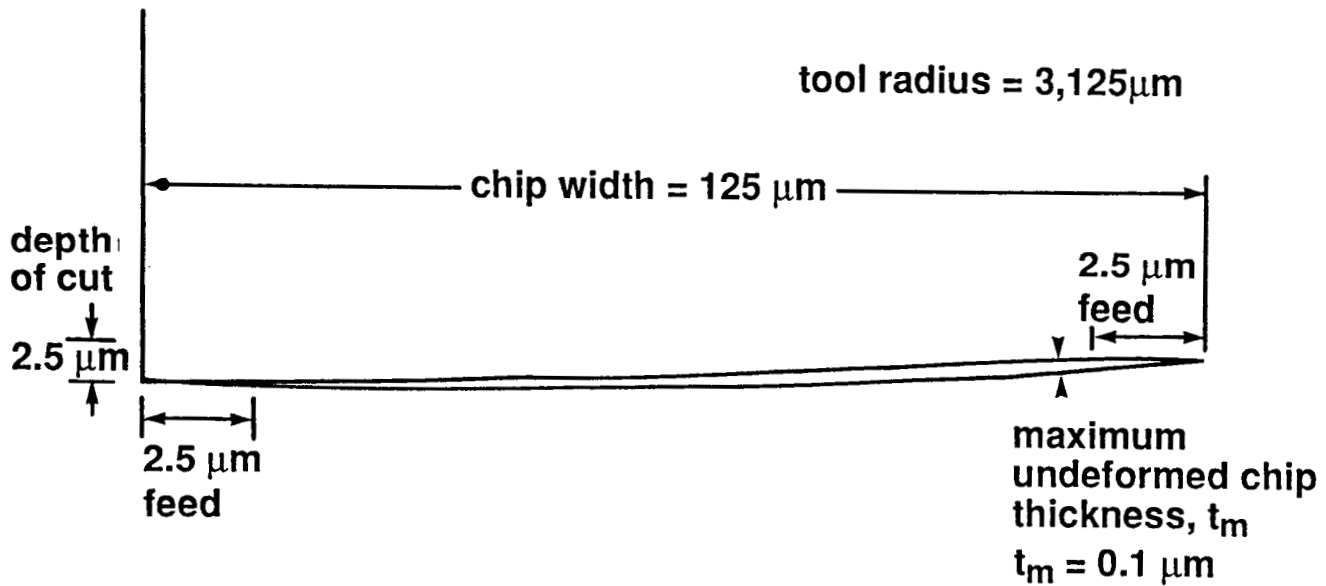


Fig. 4 Cross-section of undeformed chip geometry



Fig. 5 SEM of shoulders left when tool is lifted suddenly during facing cut. In the sample above, the tool was lifted suddenly and allowed to continue the facing for a short distance.

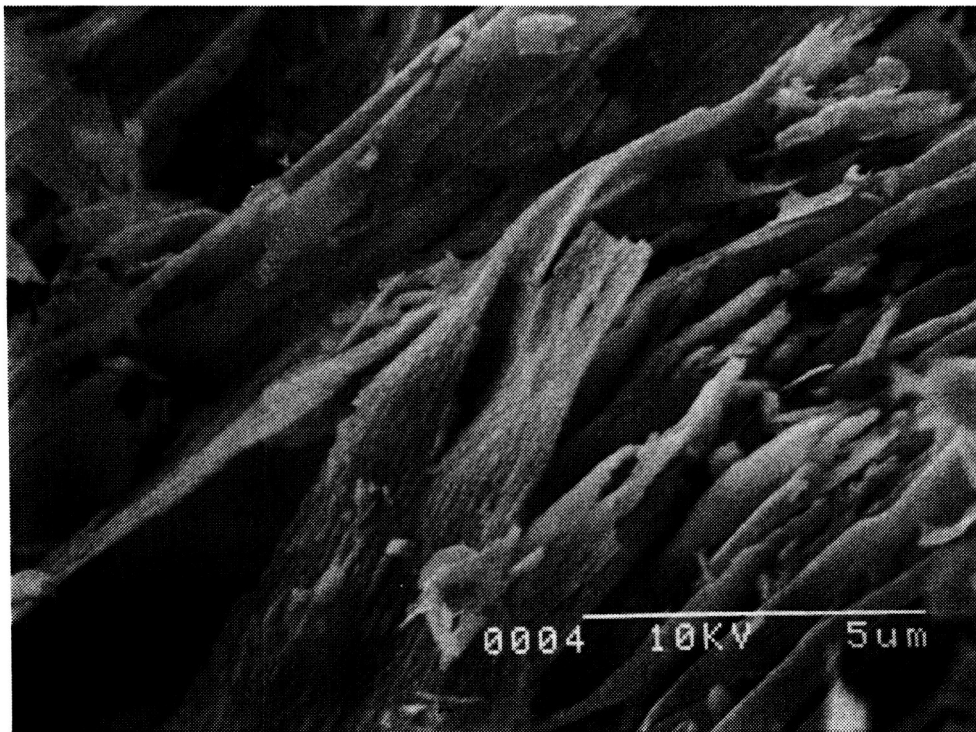


Fig. 6 Machining chips of germanium. Cut in water.

ORIGINAL PAGE IS
OF POOR QUALITY

ORIGINAL PAGE IS
OF POOR QUALITY

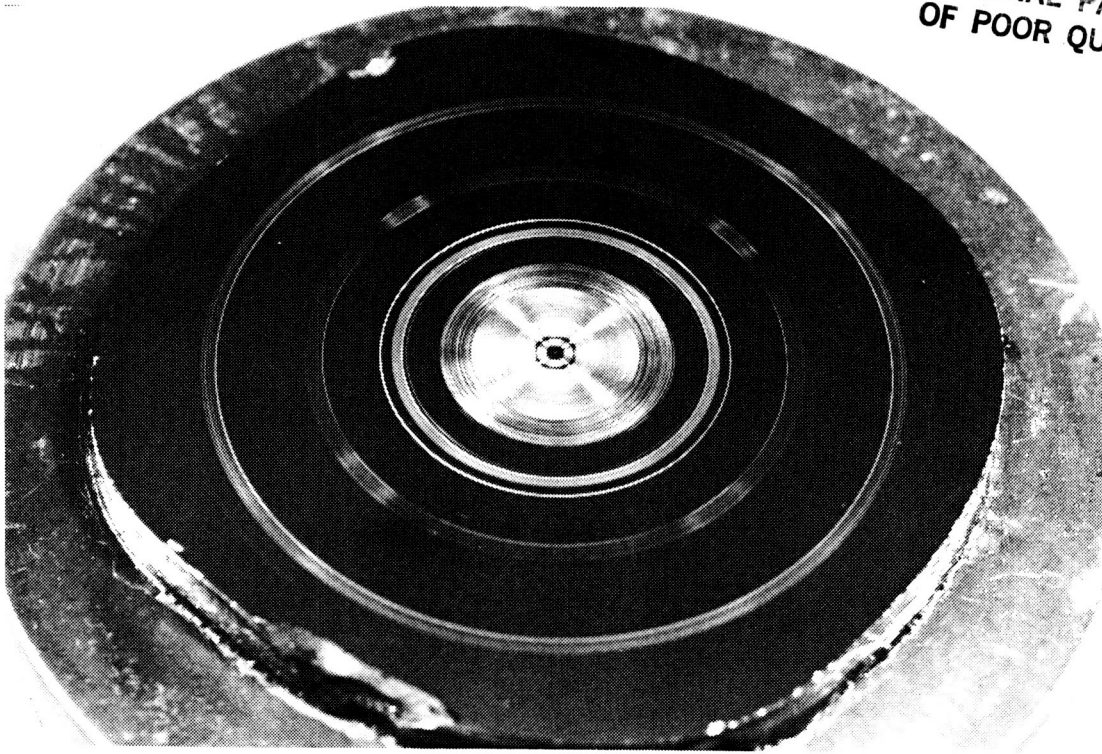


Fig. 7 Germanium disk showing finishes produced by 12 depth and feed conditions. Note the smooth areas, the light-scattering areas of pitting, and the four-fold symmetric pattern of severe pitting.

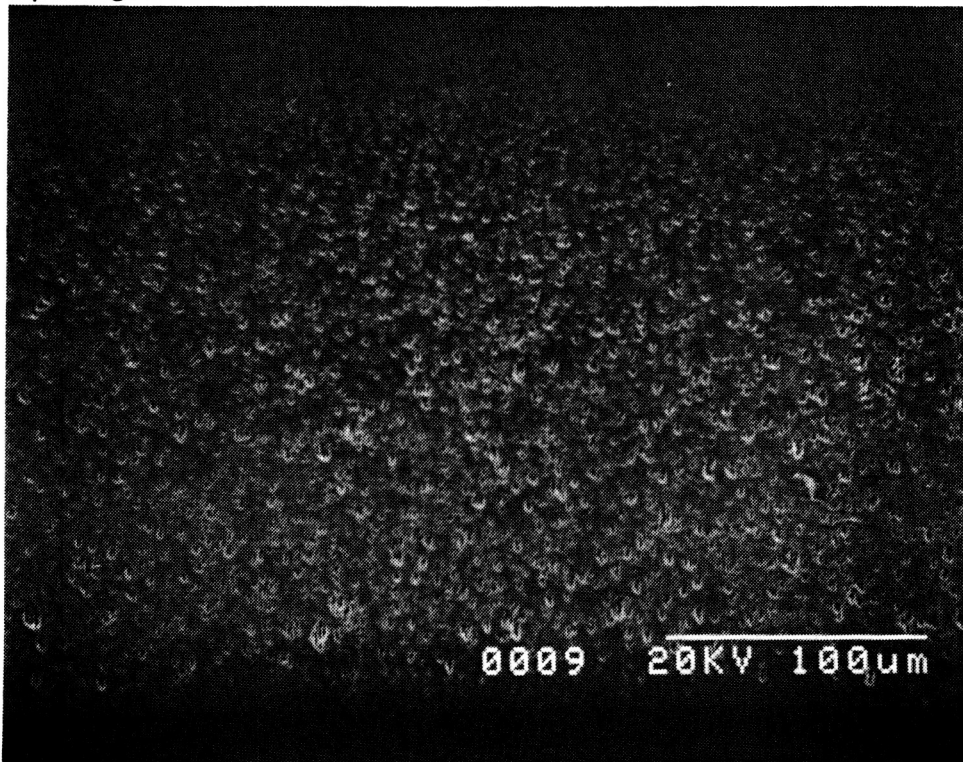


Fig. 8 Tool-lift shoulder in germanium, showing the gradation in sizes of pits as function of position on slope.

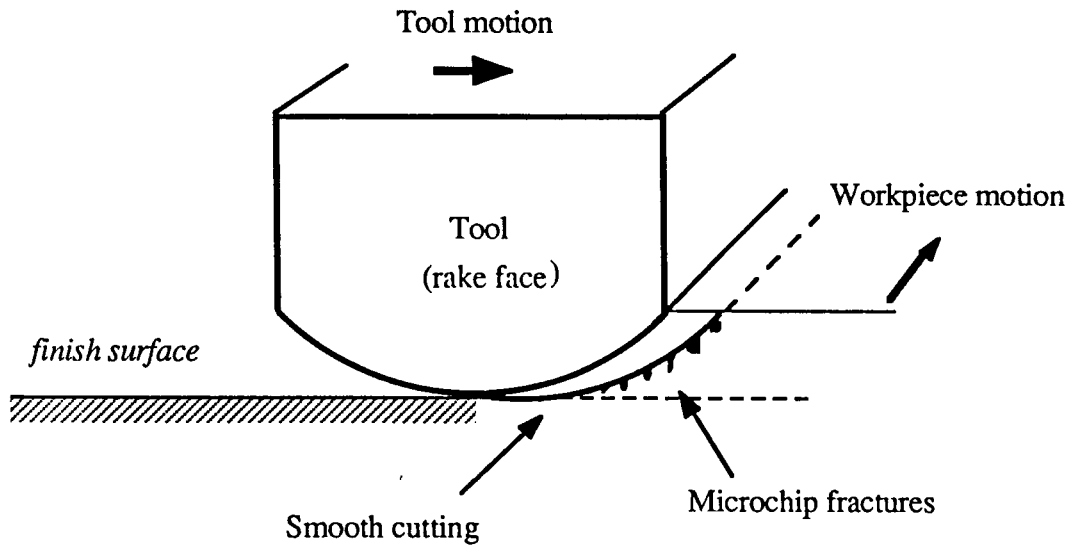


Fig. 9 Damage is created at forward edge of tool, where local thickness, t , is greater than critical value. Damage is cut off by trailing edge of tool.

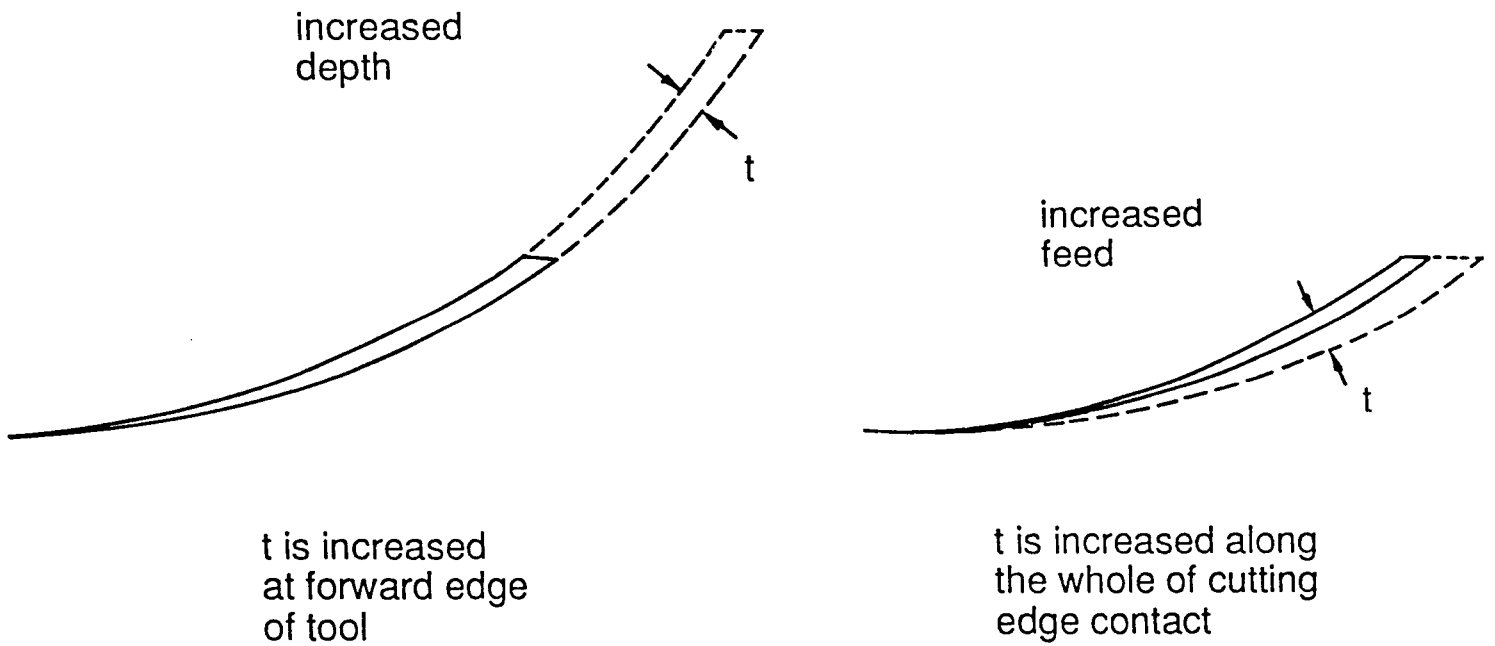


Fig. 10 The effects on the undeformed chip cross-section of increased depth and increased feed.

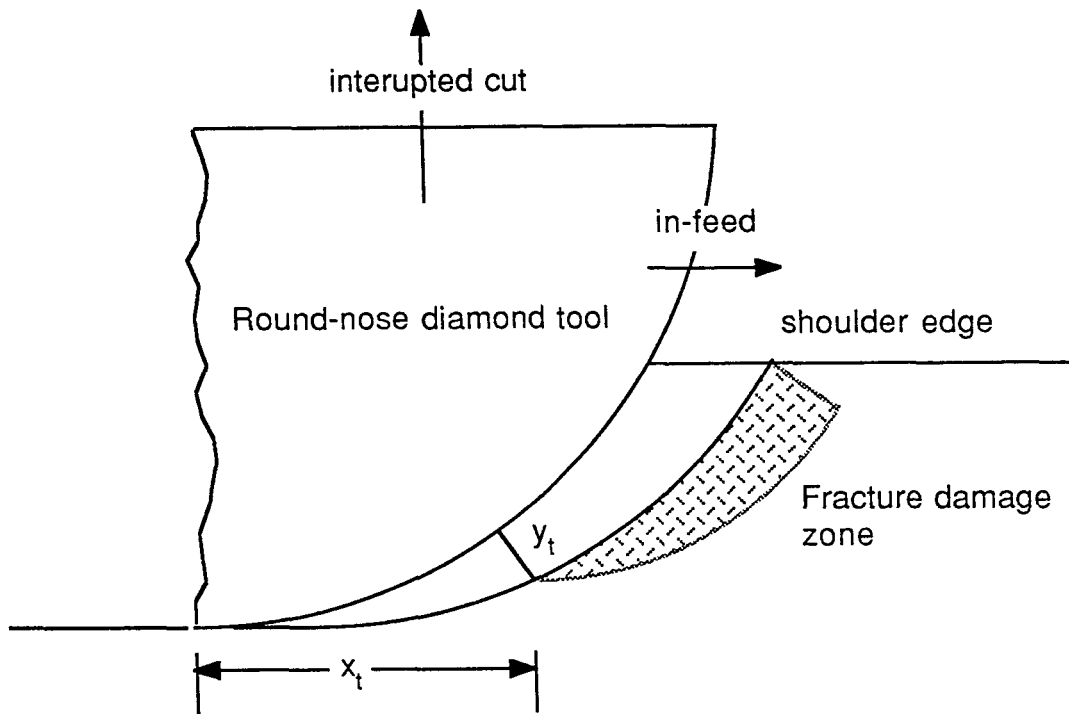


Fig. 11. Define x_t as the distance from the bottom of the tool-lift shoulder to the boundary of pitting on shoulder. Define y_t as the thickness of the chip removed from the area of the boundary of pitting.

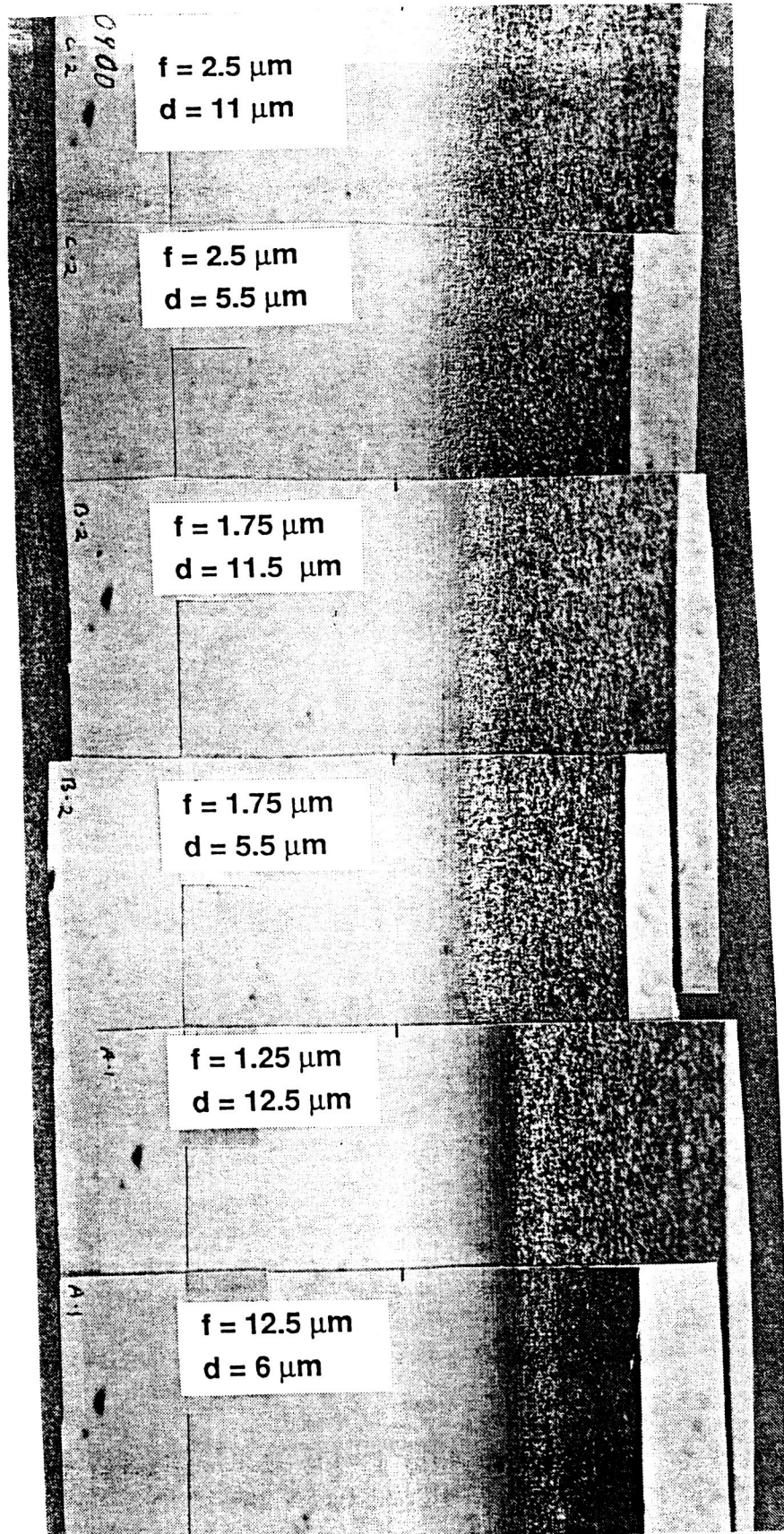


Fig. 12 Six depth and feed conditions in one workpiece of germanium. The distance up slope that pitting ceases is a function of the feed, not the depth.

Y_t vs. feed

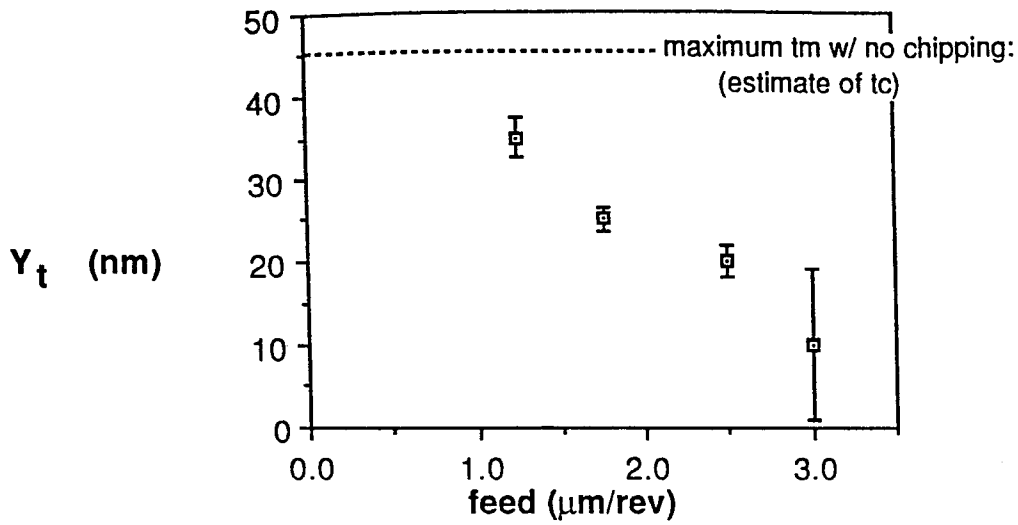


Fig. 13 Ge at 0 *deg* rake: y_t vs. feed/rev in . Estimated t_c is shown.

Y_t vs. rake angle

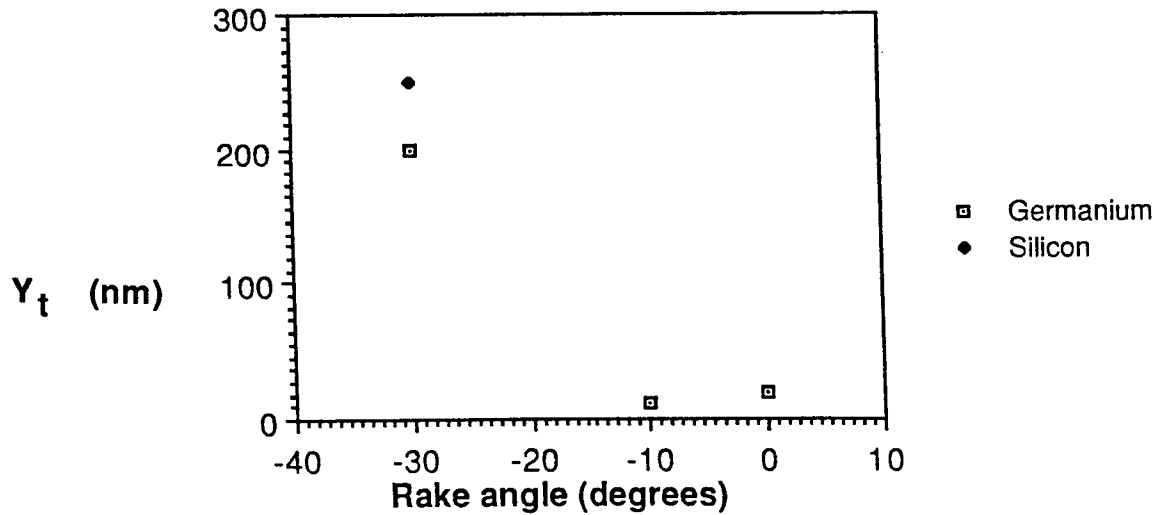


Fig 14 Graph of y_t vs. rake in Ge. Feed/rev held constant at $f = 2.5 \mu\text{m}$.

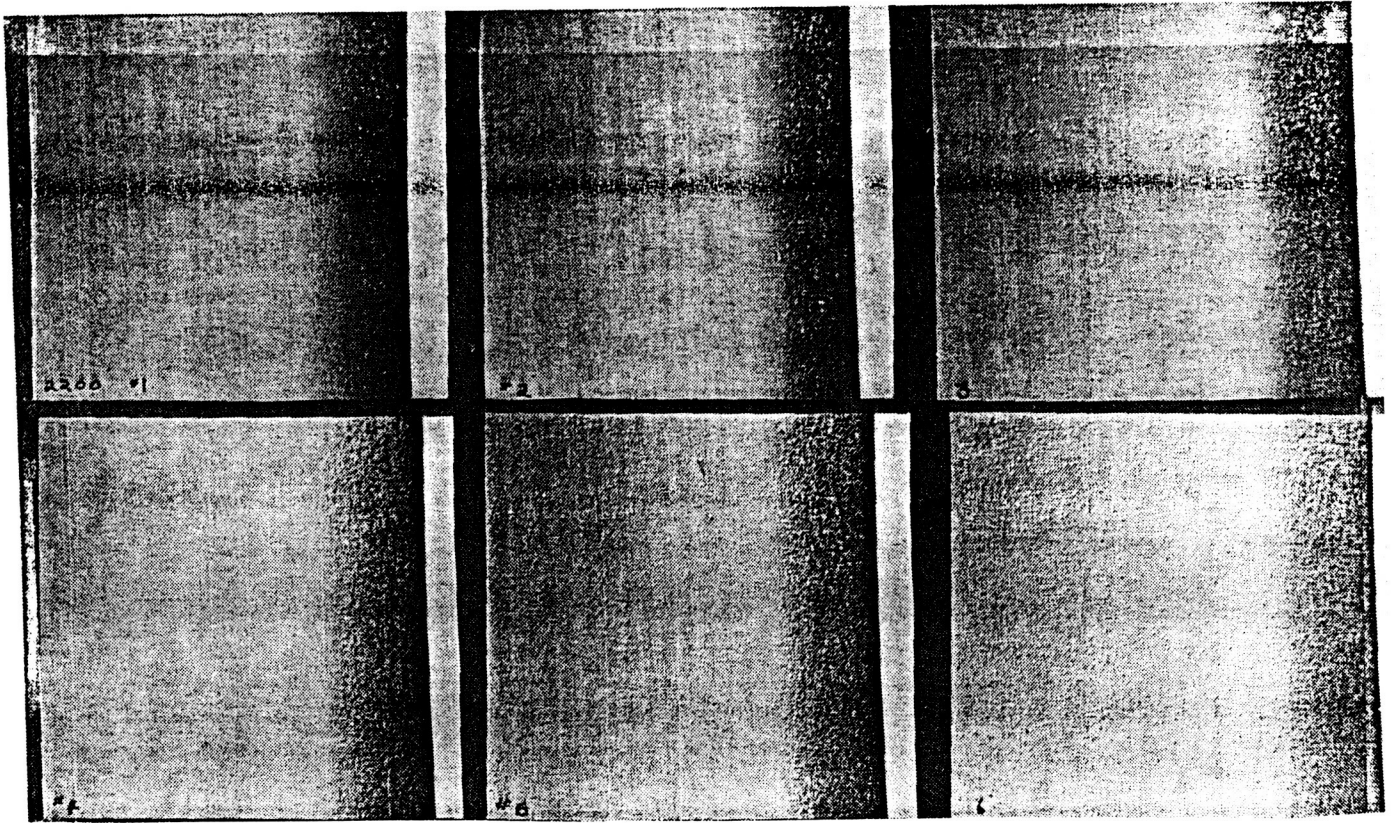


Fig. 15 Six feed and cutting speed conditions in one test on germanium. An increased cutting speed improves surface finish for given large feed.

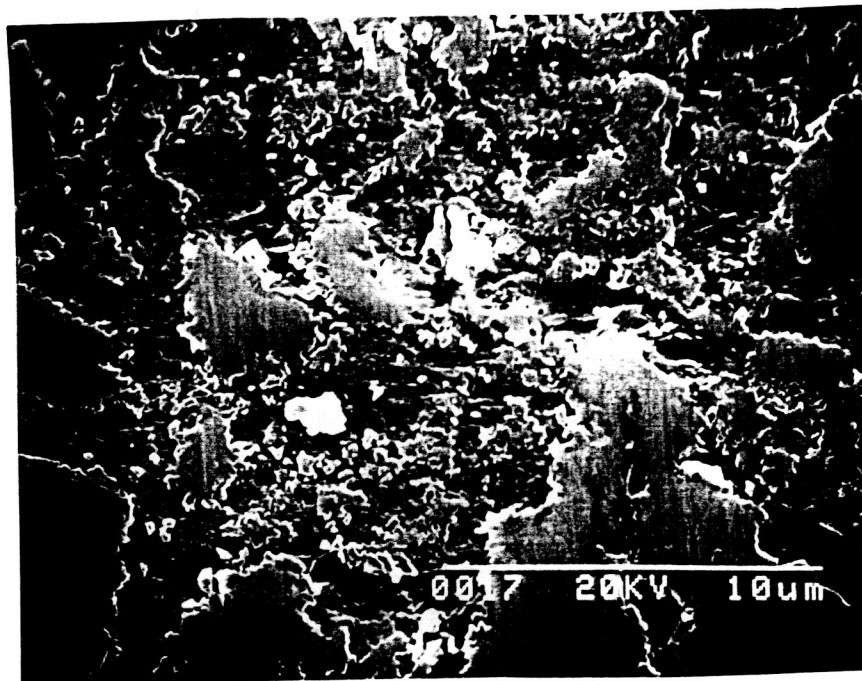


Fig. 16 Spalling damage along $\langle 100 \rangle$ in silicon.

ORIGINAL PAGE IS
OF POOR QUALITY